

# Microscopic Aspects in Dicationic Ionic Liquids through the Low-Frequency Spectra by Femtosecond Raman-Induced Kerr Effect Spectroscopy

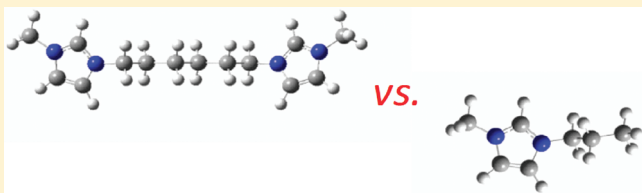
Hideaki Shirota<sup>\*,†</sup> and Tateki Ishida<sup>\*,‡</sup>

<sup>†</sup>Department of Nanomaterial Science, Graduate School of Advanced Integration Science & Department of Chemistry, Faculty of Science, Chiba University, 1-33 Yayoi, Inage-ku, Chiba 263-8522, Japan

<sup>‡</sup>Department of Theoretical and Computational Molecular Science, Institute for Molecular Science, 38 Nishigo-Naka, Myodaiji, Okazaki 444-8585, Japan

## S Supporting Information

**ABSTRACT:** The interionic vibrations in imidazolium-based dicationic ionic liquids (ILs) containing the bis(trifluoromethyl sulfonyl)amide ( $[\text{NTf}_2]^-$ ) counteranion were investigated using femtosecond optical-heterodyne-detected Raman-induced Kerr effect spectroscopy. The microscopic nature of the dicationic ILs ( $[\text{C}_n(\text{MIm})_2][\text{NTf}_2]_2$ , where  $n = 6, 10$ , and  $12$ ; MIm = *N*-methylimidazolium) was compared with that of the corresponding monocationic ILs ( $[\text{C}_n\text{MIm}][\text{NTf}_2]$ , where  $n = 3, 5$ , and  $6$ ) used as reference samples. Low-frequency Kerr spectra within the frequency range  $0\text{--}200\text{ cm}^{-1}$  of the ILs revealed that (i) the spectral profile of the dicationic ILs as well as that of the corresponding monocationic ILs is bimodal; (ii) the difference in the spectral shapes of the dicationic and monocationic ILs is greater for  $[\text{C}_6(\text{MIm})_2][\text{NTf}_2]_2$  and  $[\text{C}_3\text{MIm}][\text{NTf}_2]$  than for the ILs with longer alkylene linker/alkyl groups, namely  $[\text{C}_{10}(\text{MIm})_2][\text{NTf}_2]_2$  and  $[\text{C}_5\text{MIm}][\text{NTf}_2]$ , and  $[\text{C}_{12}(\text{MIm})_2][\text{NTf}_2]_2$  and  $[\text{C}_6\text{MIm}][\text{NTf}_2]$ ; (iii) the small difference between the dicationic and monocationic ILs is confirmed by the relative intensity of the low-frequency component (ca.  $17\text{ cm}^{-1}$ ) to the high-frequency component (ca.  $70\text{ cm}^{-1}$ ); and (iv) the spectral profiles of the three dicationic ILs are not very different, but the line-shape of the low-frequency Kerr spectrum of 1-methyl-3-propylimidazolium bis(trifluoromethylsulfonyl)amide ( $[\text{C}_3\text{MIm}][\text{NTf}_2]$ ) is significantly different from those of the other two monocationic ILs whose cations have a longer alkyl group. The distinguished line-shape of the low-frequency Kerr spectrum of  $[\text{C}_3\text{MIm}][\text{NTf}_2]$  from the other ILs can be accounted for by the homogeneous nature in the microstructure of the IL, but the other ILs indicate microsegregation structures due to the longer nonpolar alkylene linker or alkyl group in the cations.



## 1. INTRODUCTION

Ionic liquids (ILs) have many opportunities in a wide variety of applications in chemical/material science and engineering, including as replacements for volatile organic solvents in organic synthesis as well as in enzymatic reactions, electrochemistry, tribology, and radioactive-waste handling.<sup>1–9</sup> The wide applicability of ILs stems from their physical properties, which are unique for salts and liquids, such as low melting point and nonvolatility under ambient conditions. Following the development of air- and water-stable ILs by Wilkes and Zaworotko in 1992,<sup>10</sup> ILs have continued to garner increasing research interest.<sup>11–18</sup>

Monocationic ILs have been the primary target of research, but more recently, dicationic ILs have come into increasing focus because of their unique features.<sup>19–33</sup> For example, the shear viscosities, surface tensions, and liquid densities of dicationic ILs are larger than those of the corresponding monocationic ILs, which contain the same anions and comparable alkyl groups. Dicationic ILs also display remarkable thermal stability. The decomposition temperatures of dicationic ILs are  $\sim 30\text{ K}$  (or sometimes more) higher than those of the corresponding monocationic ILs.<sup>26,30–33</sup>

Therefore, high-temperature applications of dicationic ILs in lubricants,<sup>34–37</sup> stationary phases for gas chromatography,<sup>38–40</sup> solvents for high-temperature organic reactions,<sup>41</sup> electrolytes in secondary batteries,<sup>42</sup> and dye-sensitized solar cells have been proposed.<sup>43,44</sup>

The distinctive physical properties of ILs, such as low melting point and nonvolatility under ambient conditions, are largely attributed to complicated interionic interactions in these systems. Accordingly, an understanding of the microscopic (or molecular aspects of) interionic interactions in ILs is necessary. One of the most effective methods for understanding the microscopic aspects of condensed phases involves studying the intermolecular vibrational spectra whose frequency range is typically  $1\text{--}200\text{ cm}^{-1}$ ; these spectra enable us to evaluate the microscopic intermolecular interactions. Femtosecond optical-heterodyne-detected Raman-induced Kerr effect spectroscopy (OHD-RIKES) is a powerful spectroscopic technique for observing the intermolecular

**Received:** July 3, 2011

**Revised:** August 11, 2011

**Published:** August 12, 2011

vibrations in condensed phases because this spectroscopic technique can capture the molecular motions within the frequency range  $0.2\text{--}700\text{ cm}^{-1}$  with high sensitivity.<sup>45–56</sup> Recently, femtosecond OHD-RIKES has become a fundamental tool in the exploration of microscopic aspects of ILs.<sup>57–77</sup>

In this study, the interionic vibrational dynamics of imidazolium-based dicationic ILs were measured using femtosecond OHD-RIKES for the first time. Although the number of reports on dicationic ILs is increasing day by day as mentioned above, the reports on dicationic ILs are still limited, and thus the knowledge and understanding of dicationic ILs is much less than that of monocationic ILs. Some static properties, for example, shear viscosity, liquid density, and surface tension, of dicationic ILs become clearer, but the molecular-level aspects of dicationic ILs, such as interionic and intraionic vibrations and microscopic interionic interaction, and the spatial structures, such as complementary information, accessible to us are still unknown. It is reported that the presence of microsegregations in 1-alkyl-3-methylimidazolium cation-based ILs has been predicted by molecular dynamics (MD) simulations,<sup>78–82</sup> and the trace and evidence have been observed experimentally.<sup>83–85</sup> According to these studies, the microsegregations become more remarkable in the ILs containing the longer alkyl group (longer than butyl group), but the ILs having the shorter alkyl groups are rather homogeneous. These studies inspire us to investigate the microscopic aspects in dicationic ILs containing several different alkylene linkers (hexylene, decylene, and dodecylene linkers) and whether the similar trend to the monocationic IL's case will emerge even in dicationic ILs. For the comparative purposes, comparing with the monocationic ILs containing the reference alkyl groups (propyl, pentyl, and hexyl groups) and the same counteranion is also the subject in the present study to evaluate and understand both similar and distinctive characteristics of the dicationic ILs in contrast with the corresponding monocationic ILs.

## 2. EXPERIMENTAL AND QUANTUM CHEMICAL CALCULATION METHODS

The target dicationic ILs in this study are 1,6-bis(3-methylimidazolium-1-yl)hexane bis(trifluoromethylsulfonyl)amide ( $[\text{C}_6(\text{MIm})_2][\text{NTf}_2]_2$ ), 1,10-bis(3-methylimidazolium-1-yl)decane bis(trifluoromethylsulfonyl)amide ( $[\text{C}_{10}(\text{MIm})_2][\text{NTf}_2]_2$ ), and 1,12-bis(3-methylimidazolium-1-yl)dodecane bis(trifluoromethylsulfonyl)amide ( $[\text{C}_{12}(\text{MIm})_2][\text{NTf}_2]_2$ ). Their corresponding monocationic ILs are 1-methyl-3-propylimidazolium bis(trifluoromethylsulfonyl)amide ( $[\text{C}_3\text{MIm}][\text{NTf}_2]$ ), 1-methyl-3-pentylimidazolium bis(trifluoromethylsulfonyl)amide ( $[\text{C}_5\text{MIm}][\text{NTf}_2]$ ), and 1-hexyl-3-methylimidazolium bis(trifluoromethylsulfonyl)amide ( $[\text{C}_6\text{MIm}][\text{NTf}_2]$ ). The chemical structures of the cations and the anions of the sample ILs are shown in Figure 1 along with the abbreviated names of the cations and the anion. The details of the synthesis, assignments, and water contents of the ILs have been reported elsewhere.<sup>33</sup> The water contents of the ILs were within  $180\text{--}230\text{ ppm}$ .

The details of the femtosecond OHD-RIKES setup used in this study have also been reported in previous publications.<sup>52,86</sup> A laboratory-built Ti:sapphire laser based on a laser kit (CDP Systems, TISSA-kit 20) pumped by a Nd:VO<sub>4</sub> diode laser (Spectra Physics, Millennia Pro 5sJ) was used as the light source for the femtosecond OHD-RIKES setup. The output power of the Ti:sapphire laser was  $\sim 350\text{ mW}$ . The typical temporal response, which is the cross-correlation between the pump and

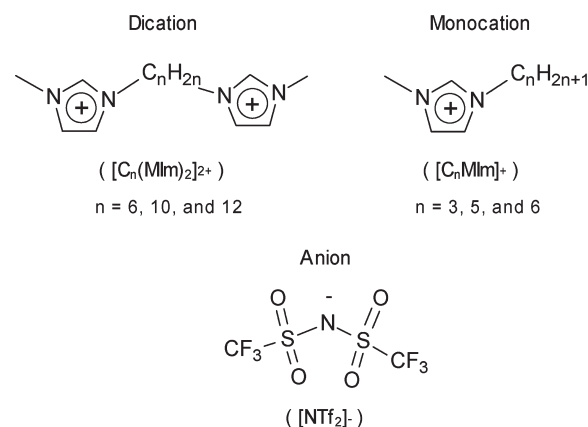


**Figure 1.** Structures and abbreviations of the cations and anion of the ILs used in this study.

probe pulses measured using a  $200\text{ }\mu\text{m}$  thick KDP crystal (type I), was  $33 \pm 3\text{ fs}$  (full width at half-maximum). Scans with a high time resolution of 2048 points at  $0.5\text{ }\mu\text{m}/\text{step}$  were performed for a short time window ( $6.8\text{ ps}$ ). Intermediate-time-window transients ( $53\text{ ps}$ ) with data acquisition of  $5.0\text{ }\mu\text{m}/\text{step}$  and long-time-window transients ( $300\text{ ps}$ ) with data acquisition of  $50.0\text{ }\mu\text{m}/\text{step}$  were also captured. Obtaining pure heterodyne signals was achieved by recording scans for both  $+\sim 1^\circ$  and  $-\sim 1^\circ$  rotations of the input polarizer; these were then combined to eliminate the residual homodyne signal. The ILs were injected into a quartz cell with an optical path length of  $3\text{ mm}$  (Tosoh Quartz) via a  $0.2\text{ }\mu\text{m}$  Anotop filter (Whatman) prior to the femtosecond OHD-RIKES measurements. All OHD-RIKES measurements were performed at  $296 \pm 1\text{ K}$ .

The optimized structures and their normal modes of the two cations, that is,  $[\text{C}_6(\text{MIm})_2]^{2+}$  and  $[\text{C}_3\text{MIm}]^+$ , and the anion  $[\text{NTf}_2]^-$  were determined from ab initio quantum chemical calculations based on the B3LYP/aug-cc-pVTZ level of theory,<sup>87–91</sup> carried out using the Gaussian 03 program suite.<sup>92</sup> The obtained atom coordinates, dipole moments, polarizability tensor elements, mean polarizabilities, and polarizability anisotropy volumes of the ions are summarized in the Supporting Information.

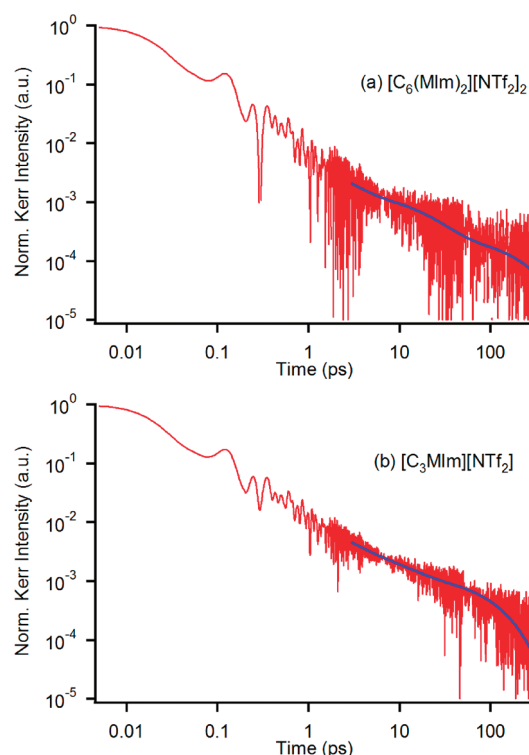
## 3. RESULTS

**3.1. Static Physical Properties.** Some static physical properties of the dicationic and monocationic ILs studied herein have been previously published.<sup>33</sup> The reported data for the liquid densities, molar volumes, decomposition temperatures, shear viscosities, and surface tensions of the target ILs are summarized in Table 1 for comparison with the dynamical data presented in Section 3.2.<sup>33</sup> As shown in Table 1, the notable features of the dicationic ILs that emerge upon comparison with the corresponding monocationic ILs are (i) the liquid densities of the dicationic ILs are larger, (ii) the decomposition temperatures are higher, (iii) the shear viscosities are higher, and (iv) the surface tensions are larger than those of the corresponding monocationic ILs.

**3.2. Ultrafast Dynamics.** Figure 2 shows the logarithmic plots of the Kerr transients for  $[\text{C}_6(\text{MIm})_2][\text{NTf}_2]_2$  and  $[\text{C}_3\text{MIm}][\text{NTf}_2]$  as representative examples. In the time region ranging from  $50\text{ fs}$  to several picoseconds, strong beating trajectories are observed in the Kerr transients for not only  $[\text{C}_6(\text{MIm})_2][\text{NTf}_2]_2$  and  $[\text{C}_3\text{MIm}][\text{NTf}_2]$  but also the other ILs. For the longest time

**Table 1.** Molecular Weights, MW, Liquid Densities,  $d$ , Molar Volumes,  $V_m$ , Shear Viscosities,  $\eta$ , and Surface Tensions,  $\gamma$ , at 297 K of Dicationic and Monocationic ILs

IL	MW	$d$ (g/cm <sup>3</sup> )	$V_m$ (cm <sup>3</sup> /mol)	$T_d$ (K)	$\eta$ (cP)	$\gamma$ (mN/m)
[C <sub>6</sub> (MIm) <sub>2</sub> ][NTf <sub>2</sub> ] <sub>2</sub>	808.7	1.546	523.1	700.1	649.5	41.1
[C <sub>10</sub> (MIm) <sub>2</sub> ][NTf <sub>2</sub> ] <sub>2</sub>	864.8	1.462	591.5	689.4	720.6	39.4
[C <sub>12</sub> (MIm) <sub>2</sub> ][NTf <sub>2</sub> ] <sub>2</sub>	892.8	1.428	625.2	681.3	842.4	38.6
[C <sub>3</sub> MIm][NTf <sub>2</sub> ]	405.0	1.476	274.4	672.0	42.8	35.9
[C <sub>5</sub> MIm][NTf <sub>2</sub> ]	433.1	1.403	308.7	670.4	59.1	34.0
[C <sub>6</sub> MIm][NTf <sub>2</sub> ]	447.1	1.373	325.6	635.4	69.3	33.8

**Figure 2.** Log–log plots of Kerr transients of (a) [C<sub>6</sub>(MIm)<sub>2</sub>][NTf<sub>2</sub>]<sub>2</sub> and (b) [C<sub>3</sub>MIm][NTf<sub>2</sub>]. Triexponential fits to the Kerr transients are shown by blue lines.

scale in the Kerr transients, a triexponential function is used to fit the data within the time range 3–270 ps. In addition to multiexponential function fits, a practical function on the basis of the mode coupling theory has also been used to characterize the overdamped decays in ILs.<sup>93,94</sup> However, the time constants of the  $\alpha$ -relaxation process (the slowest relaxation) in ILs are mostly longer than the observed time range in this study, and such cases result in a large uncertainty in the fit parameters.<sup>62</sup> Accordingly, we used triexponential functions for data fitting in this study. The triexponential fits are also shown in Figure 2. The fitting parameters for all ILs studied herein are summarized in Table 2. As shown in Figure 2 and Table 2, the slow relaxation time ( $\tau_3$ ) of the dicationic ILs is almost independent of the alkylene linker in the dications. Similarly,  $\tau_3$  of the monocationic ILs does not vary, irrespective of the alkyl group in the monocations. However,  $\tau_3$  of the dicationic ILs is much slower than that of the monocationic ILs. This feature can possibly be attributed to the marked difference in the shear viscosity between the dicationic ILs and the monocationic ILs (Table 1). The fast

and intermediate relaxation times ( $\tau_1$  and  $\tau_2$ ) are not very different among the ILs. A similar feature has also been reported in the overdamped relaxation processes in various monocationic ILs.<sup>59,61–66</sup>

Figure 3 shows the short-time-range Kerr transients of (a) the dicationic ILs and (b) the monocationic ILs. To facilitate a critical comparison of the dicationic and monocationic ILs, we present the short-time-range Kerr transients for [C<sub>6</sub>(MIm)<sub>2</sub>][NTf<sub>2</sub>]<sub>2</sub> and [C<sub>3</sub>MIm][NTf<sub>2</sub>] in Figure 3c as a representative example. As shown in the Figures, the differences in the Kerr transients among the dicationic ILs containing various alkylene linker lengths (Figure 3a) and the monocationic ILs containing different alkyl group lengths (Figure 3b) are small. Comparison of [C<sub>6</sub>(MIm)<sub>2</sub>][NTf<sub>2</sub>]<sub>2</sub> with [C<sub>3</sub>MIm][NTf<sub>2</sub>] shows that the relative Kerr signal intensity of the nuclear response to the electronic response ( $t = 0$ ) in the earlier time stage (50 to 200 fs) of [C<sub>6</sub>(MIm)<sub>2</sub>][NTf<sub>2</sub>]<sub>2</sub> is lower than that of [C<sub>3</sub>MIm][NTf<sub>2</sub>], and the damped feature of the Kerr transients is quite similar for the two ILs. It can be expected that this difference in the Kerr transient arises from a variation in the interionic vibrations because the interionic (or intermolecular) vibrations contribute largely to the intensity of the Kerr signal in this time region.

Low-frequency Kerr spectra were obtained by the standard Fourier transform deconvolution analysis of the Kerr transients, a method that has been established by McMorro and Lotshaw.<sup>95,96</sup> Figures 4 and 5 show the Fourier transform Kerr spectra of the dicationic and monocationic ILs, respectively. The Kerr spectra without the contributions from the overdamped picosecond relaxation processes (second and third exponential components) are also shown to highlight the vibrational contributions: these spectra were used for the line-shape analysis according to traditional OHD-RIKES experiments. The contribution of the overdamped picosecond relaxation processes in each IL is also shown in Figures 4 and 5. The spectra represent well up to  $\sim 750$  cm<sup>−1</sup>, as seen in the Figures.

There are two different types of vibrational bands in the Kerr spectra of the ILs. These two bands can be attributed to the intraionic vibrational modes and the interionic vibrational band, respectively. The former band is rather sharp, whereas the latter is broad and in the low-frequency region below 200 cm<sup>−1</sup>. As seen in Figures 4 and 5, the intraionic vibrational modes of the dicationic ILs are quite similar to those of the monocationic ILs. The intra-molecular vibrational modes and their assignments are summarized in the Supporting Information.

The broad spectral bands below 200 cm<sup>−1</sup> for the ILs were further subjected to line-shape analysis to reproduce and characterize the broad and complicated spectral shape. The fit function

**Table 2.** Triexponential Fit Parameters for Kerr Transients in Dicationic and Monocationic ILs

IL	$a_1$	$\tau_1$ (ps)	$a_2$	$\tau_2$ (ps)	$a_3$	$\tau_3$ (ps)
[C <sub>6</sub> (MIm) <sub>2</sub> ][NTf <sub>2</sub> ] <sub>2</sub>	0.00397 ± 0.00123	1.83 ± 0.45	0.00117 ± 0.00015	16.5 ± 4.4	0.00028 ± 0.00011	185.1 ± 95.0
[C <sub>10</sub> (MIm) <sub>2</sub> ][NTf <sub>2</sub> ] <sub>2</sub>	0.00254 ± 0.00101	1.91 ± 0.63	0.00094 ± 0.00013	17.6 ± 5.6	0.00030 ± 0.00011	182.4 ± 86.2
[C <sub>12</sub> (MIm) <sub>2</sub> ][NTf <sub>2</sub> ] <sub>2</sub>	0.00260 ± 0.00039	2.71 ± 0.84	0.00063 ± 0.00040	12.7 ± 8.6	0.00020 ± 0.00008	173.7 ± 101.0
[C <sub>3</sub> MIm][NTf <sub>2</sub> ]	0.00875 ± 0.00183	1.71 ± 0.37	0.00258 ± 0.00061	8.07 ± 1.56	0.00127 ± 0.00008	96.6 ± 8.3
[C <sub>5</sub> MIm][NTf <sub>2</sub> ]	0.00546 ± 0.00044	2.53 ± 0.41	0.00112 ± 0.00040	12.0 ± 5.2	0.00070 ± 0.00013	96.1 ± 17.2
[C <sub>6</sub> MIm][NTf <sub>2</sub> ]	0.00470 ± 0.00074	2.11 ± 0.45	0.00124 ± 0.00034	11.2 ± 3.5	0.00065 ± 0.00008	119.2 ± 18.8

for the low-frequency Kerr spectra used in this study is a sum of Ohmic (eq 1) and antisymmetrized Gaussian functions (eq 2)<sup>97</sup>

$$I_O(\omega) = a_O \omega \exp(-\omega/\omega_O) \quad (1)$$

$$I_G(\omega) = \sum_{i=1}^3 \left\{ a_{G,i} \exp \left[ \frac{-2(\omega - \omega_{G,i})^2}{\Delta\omega_{G,i}^2} \right] - a_{G,i} \exp \left[ \frac{-2(\omega + \omega_{G,i})^2}{\Delta\omega_{G,i}^2} \right] \right\} \quad (2)$$

where  $a_O$  and  $\omega_O$  are the amplitude and characteristic frequency parameters of the Ohmic line-shape, respectively;  $a_{G,i}$ ,  $\omega_{G,i}$ , and  $\Delta\omega_{G,i}$  are the amplitude, characteristic frequency, and bandwidth parameters for the  $i$ th antisymmetrized Gaussian function, respectively. A Lorentzian function (eq 3) was used when a clear intraionic vibrational band was observed in the Kerr spectra

$$I_L(\omega) = \frac{a_L}{(\omega - \omega_L)^2 + \Delta\omega_L^2} \quad (3)$$

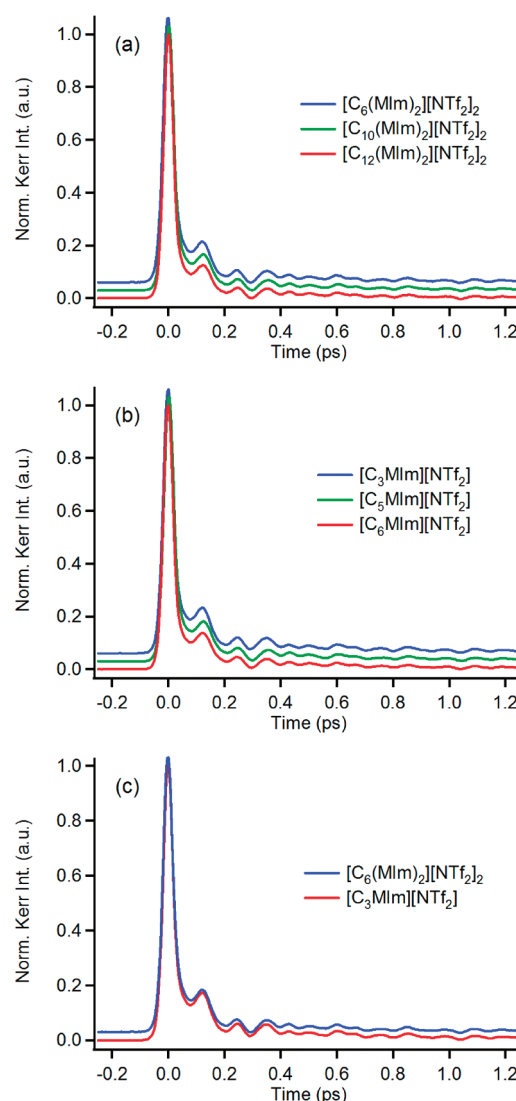
where  $a_L$ ,  $\omega_L$ , and  $\Delta\omega_L$  are the amplitude, peak frequency, and bandwidth parameters for the Lorentzian function, respectively.

Figure 6 shows the results of the line-shape analysis for the low-frequency Kerr spectra of the dicationic and monocationic ILs. Several clear intraionic vibrational bands were confirmed in the low-frequency Kerr spectra, as shown in the Figure. The vibrational bands were assigned on the basis of quantum chemical calculations (Section 3.3). The vibrational bands at ca. 170 and 215 cm<sup>-1</sup> are assigned to the cation, and the band at ~120 cm<sup>-1</sup> is attributed to the anion. Table 3 summarizes the fit parameters for the line-shape analysis. In Table 3, the first spectral moments  $M_1$  of the low-frequency Kerr spectra without the contributions of clear intraionic vibrational modes and picosecond overdamped relaxation for the ILs are also summarized.  $M_1$  is defined as

$$M_1 = \int \omega I(\omega) d\omega / \int I(\omega) d\omega \quad (4)$$

where  $I(\omega)$  is the frequency-dependent spectral intensity. Note that the fit parameters of the model functions (eqs 1 and 2) are covariant, and the broad spectrum has no clear peak except for intraionic vibrational modes, and thus the fit parameters include rather large errors, as shown in Table 3.

The low-frequency Kerr spectra of the dicationic and monocationic ILs shown in Figure 6 illustrate the following noteworthy points: (i) the spectral profile is bimodal (with maxima at ca. 17 and 70 cm<sup>-1</sup>) for both the dicationic and monocationic ILs; (ii) the difference in the spectral shapes between the dicationic and monocationic ILs is larger for [C<sub>6</sub>(MIm)<sub>2</sub>][NTf<sub>2</sub>]<sub>2</sub> vs [C<sub>3</sub>MIm][NTf<sub>2</sub>] than for the ILs with longer alkylene linker/alkyl group, namely, [C<sub>10</sub>(MIm)<sub>2</sub>][NTf<sub>2</sub>]<sub>2</sub> vs [C<sub>5</sub>MIm][NTf<sub>2</sub>] and



**Figure 3.** Short-time-window Kerr transients of (a) dicationic ILs ([C<sub>6</sub>(MIm)<sub>2</sub>][NTf<sub>2</sub>]<sub>2</sub>; blue; [C<sub>10</sub>(MIm)<sub>2</sub>][NTf<sub>2</sub>]<sub>2</sub>; green; [C<sub>12</sub>(MIm)<sub>2</sub>][NTf<sub>2</sub>]<sub>2</sub>; red) and (b) monocationic ILs ([C<sub>3</sub>MIm][NTf<sub>2</sub>]; blue; [C<sub>5</sub>MIm][NTf<sub>2</sub>]; green; [C<sub>6</sub>MIm][NTf<sub>2</sub>]; red). (c) Comparison of a dicationic IL ([C<sub>6</sub>(MIm)<sub>2</sub>][NTf<sub>2</sub>]<sub>2</sub>; blue) and a monocationic IL ([C<sub>3</sub>MIm][NTf<sub>2</sub>]; red) is also shown.

[C<sub>12</sub>(MIm)<sub>2</sub>][NTf<sub>2</sub>]<sub>2</sub> vs [C<sub>6</sub>MIm][NTf<sub>2</sub>]; (iii) the relative intensity of the low-frequency component (ca. 17 cm<sup>-1</sup>) to the higher-frequency (ca. 70 cm<sup>-1</sup>) is slightly smaller for the dicationic IL than the corresponding monocationic IL; and (iv) the spectral profiles of the three dicationic ILs are not very different, but the line-shape of the low-frequency Kerr spectrum of [C<sub>3</sub>MIm][NTf<sub>2</sub>]



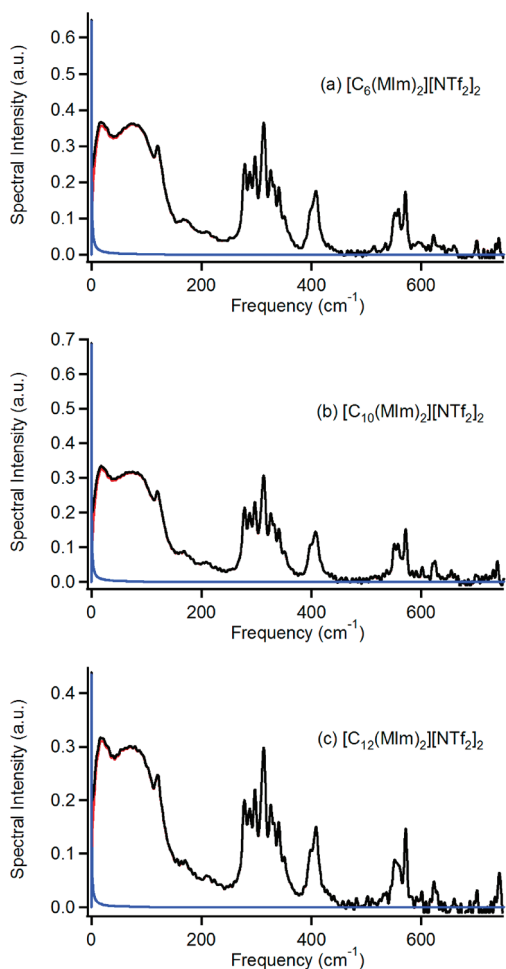
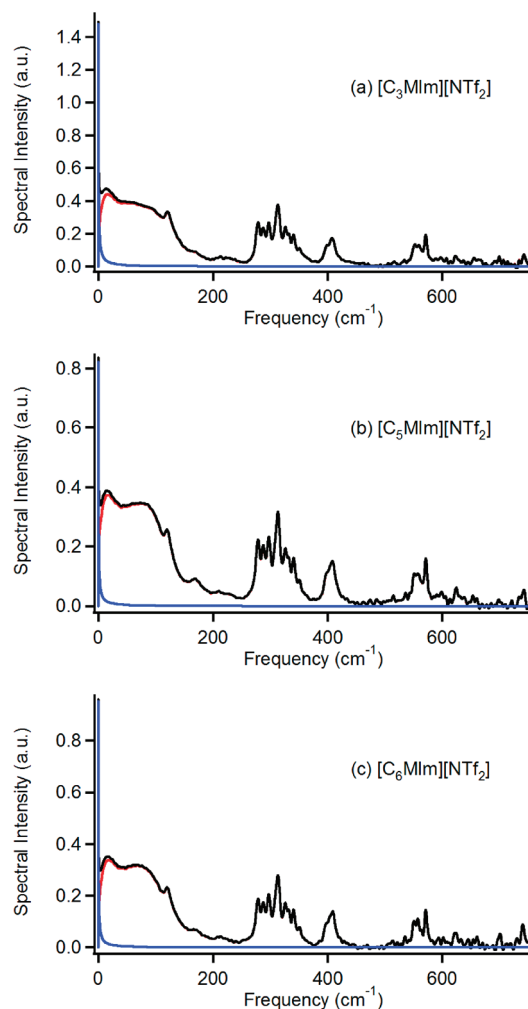


**Figure 4.** Fourier transform Kerr spectra within the frequency range 0–750  $\text{cm}^{-1}$  in the dicationic ILs: (a)  $[\text{C}_6(\text{MIm})_2][\text{NTf}_2]_2$ , (b)  $[\text{C}_{10}(\text{MIm})_2][\text{NTf}_2]_2$ , and (c)  $[\text{C}_{12}(\text{MIm})_2][\text{NTf}_2]_2$ . Black denotes the whole spectrum, blue denotes the component of the overdamped picoseconds relaxation component, and red denotes the spectrum without the component of the overdamped picoseconds relaxation.

is distinctly different from those of the other two monocationic ILs. These unique features of the low-frequency Kerr spectra of the dicationic and monocationic ILs will be discussed in more depth in Section 4.

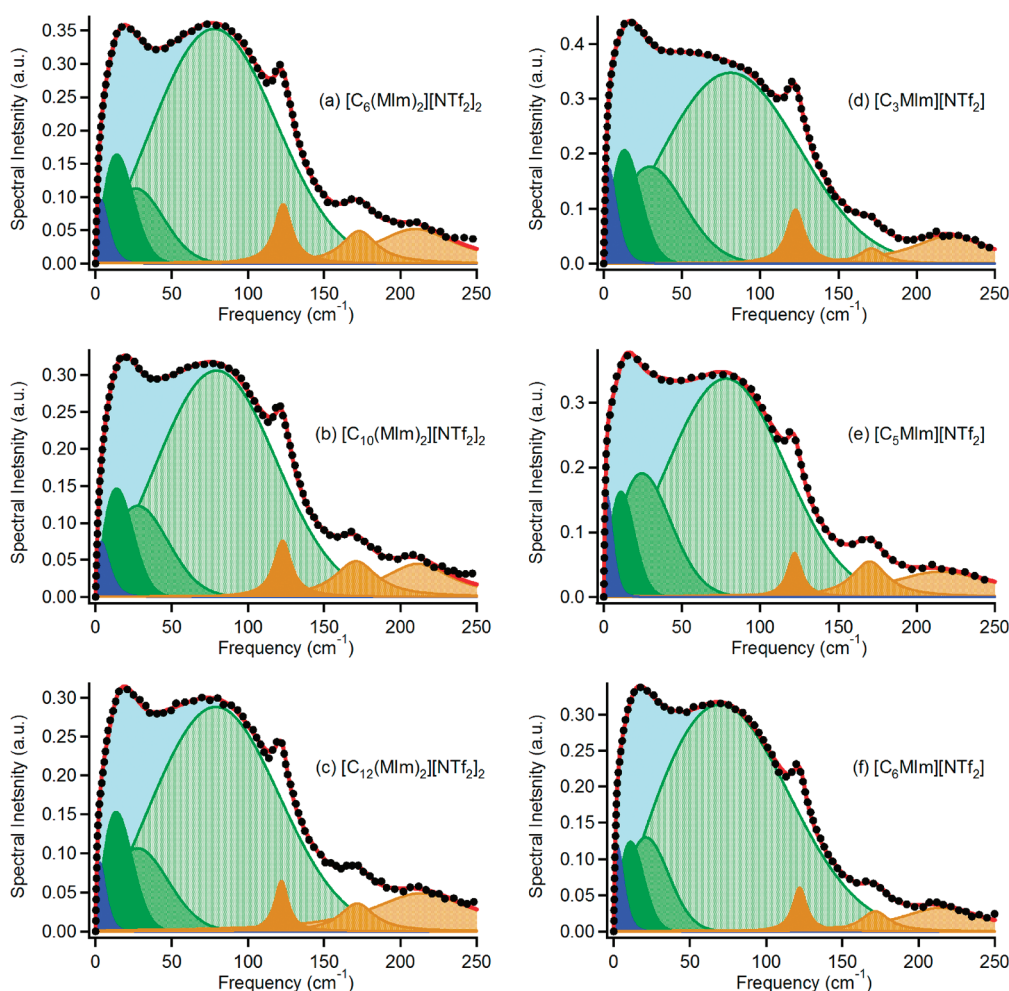
**3.3. Ab Initio Quantum Chemical Calculations.** Figure 7 shows the optimized structures of  $[\text{C}_6(\text{MIm})_2]^{2+}$  and  $[\text{C}_3\text{MIm}]^+$  based on the B3LYP/aug-cc-pVTZ level of theory. The dipole moment, mean polarizability, and polarizability anisotropy volume of the optimized  $[\text{C}_6(\text{MIm})_2]^{2+}$  cation are 1.848 D, 27.671  $\text{\AA}^3$ , and 16.817  $\text{\AA}^3$ , respectively, and those of the optimized  $[\text{C}_3\text{MIm}]^+$  are 3.479 D, 13.818  $\text{\AA}^3$ , and 7.026  $\text{\AA}^3$ , respectively. (See the Supporting Information.) The hexylene linker of the optimized  $[\text{C}_6(\text{MIm})_2]^{2+}$  is in the all-*trans* form. In contrast with the present result, the results of the ab initio quantum chemical calculations performed by Bodo and Caminiti at the CAM-B3LYP/6-31G(d) level show stable entangled structures of imidazolium-type dications.<sup>98</sup> This difference in the optimized structures of the dications likely arises from the presence/absence of the anions.

Figure 8 shows the calculated Raman spectra of (a)  $[\text{C}_6(\text{MIm})_2]^{2+}$  and (b)  $[\text{C}_3\text{MIm}]^+$ . The calculated Raman spectrum of  $[\text{NTf}_2]^-$  determined by ab initio quantum chemical calculations is also



**Figure 5.** Fourier transform Kerr spectra within the frequency range 0–750  $\text{cm}^{-1}$  in the monocationic ILs: (a)  $[\text{C}_3\text{MIm}][\text{NTf}_2]$ , (b)  $[\text{C}_5\text{MIm}][\text{NTf}_2]$ , and (c)  $[\text{C}_6\text{MIm}][\text{NTf}_2]$ . Black denotes the whole spectrum, blue denotes the component of the overdamped picoseconds relaxation component, and red denotes the spectrum without the component of the overdamped picoseconds relaxation.

shown in Figure 8c. The Raman spectra of  $[\text{C}_6(\text{MIm})_2]^{2+}$  and  $[\text{C}_3\text{MIm}]^+$  are only similar in the frequency range above 600  $\text{cm}^{-1}$ . A significant difference between the two cations is that a vibrational band is clear at 360  $\text{cm}^{-1}$  in the case of  $[\text{C}_3\text{MIm}]^+$  and at 170  $\text{cm}^{-1}$  for  $[\text{C}_6(\text{MIm})_2]^{2+}$ . The 360  $\text{cm}^{-1}$  band of  $[\text{C}_3\text{MIm}]^+$  is derived from the bending mode of the methylene part of the propyl group, which is attached to the nitrogen of the imidazolium ring, and the 170  $\text{cm}^{-1}$  band of  $[\text{C}_6(\text{MIm})_2]^{2+}$  is derived from the accordion motion of the entire ion. In fact, these bands are not clearly observed in the experimentally obtained Kerr spectra of  $[\text{C}_6(\text{MIm})_2][\text{NTf}_2]_2$  and  $[\text{C}_3\text{MIm}][\text{NTf}_2]$  (Figures 4a and 5a), possibly because these vibrational modes are not strongly depolarized or because the alkylene linker and alkyl group of the cations are not actually in the all-*trans* form in the liquid state. Many strong intraionic vibrational bands are also present within the frequency range 100–600  $\text{cm}^{-1}$  in the Kerr spectrum of the imidazolium-based ILs; these bands are attributable to the  $[\text{NTf}_2]^-$  anion.<sup>59,61,62,64,66,76</sup>



**Figure 6.** Low-frequency Kerr spectra within the frequency range 0–250  $\text{cm}^{-1}$  and fit functions for (a)  $[\text{C}_6(\text{MIm})_2][\text{NTf}_2]_2$ , (b)  $[\text{C}_{10}(\text{MIm})_2][\text{NTf}_2]_2$ , (c)  $[\text{C}_{12}(\text{MIm})_2][\text{NTf}_2]_2$ , (d)  $[\text{C}_3\text{MIm}][\text{NTf}_2]$ , (e)  $[\text{C}_5\text{MIm}][\text{NTf}_2]$ , and (f)  $[\text{C}_6\text{MIm}][\text{NTf}_2]$ . Black dots denote the experimentally obtained spectra, red solid lines denote the entire fits, blue areas denote the Ohmic functions (eq 1), green areas (dark, medium, and light green) denote the antisymmetrized Gaussian functions (eq 2), brown areas (dark, medium, and light brown) denote the Lorentzian functions (eq 3) for the intraionic vibrational modes, and light-blue areas denote the interionic contributions (sum of eqs 1 and 2).

#### 4. DISCUSSION

Although some intraionic vibrational modes minorly contribute to the spectral band in the case of ILs including relatively large ions, the main contributions to the broad band within the frequency range 0–200  $\text{cm}^{-1}$  in ILs are the interionic vibrations. The interionic vibrational spectrum probes the microscopic interionic interactions, and thus it is important to understand the details of the low-frequency vibrational spectra of ILs. In this study, we concentrate particularly on the following points of the interionic vibrations in the dicationic ILs: (i) common features of low-frequency Kerr spectra of imidazolium-based ILs containing the  $[\text{NTf}_2]^-$  anion, (ii) comparison of low-frequency Kerr spectra between dicationic and monocationic ILs, (iii) dependences of the low-frequency Kerr spectrum on the alkylene linker and alkyl group of dication and monocation, and (iv) comparison of the low-frequency Kerr spectrum with the bulk properties.

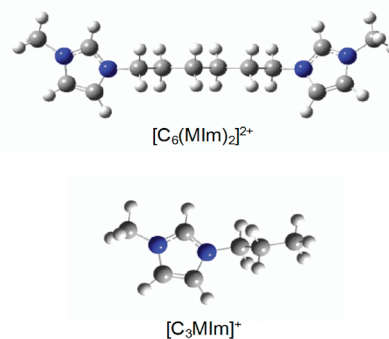
**4.1. Line-Shape of Low-Frequency Spectrum in Imidazolium-Based ILs with  $[\text{NTf}_2]^-$ .** At first, a brief review of the line-shape features of imidazolium-based ILs containing the  $[\text{NTf}_2]^-$  anion is necessary to clarify the commonly observed features of the spectral profiles of the ILs. As mentioned in Section 3.2, the

line-shape of the low-frequency Kerr spectra for all ILs studied herein is bimodal (Figure 6). In fact, this is a general feature of aromatic monocation-based ILs containing the  $[\text{NTf}_2]^-$  anion.<sup>59,61,62,64,66,76</sup> Nonaromatic ILs containing the  $[\text{NTf}_2]^-$  anion exhibit a triangular spectral shape.<sup>59,65</sup> The broad and strong band at 70  $\text{cm}^{-1}$  in the imidazolium ILs can be attributed to the librational motion of the imidazolium ring because the librational motion in neutral aromatic molecular liquids is  $\sim 60 \text{ cm}^{-1}$  and is anisotropic and strongly Raman-active.<sup>52,86,99–104</sup> This consideration is supported by the finding that several MD simulations for imidazolium-based ILs show strong intermolecular vibrational bands in the high-frequency region of approximately 50–100  $\text{cm}^{-1}$  as a result of imidazolium-ring librational motion or related motion.<sup>105–108</sup>

In addition to the features of the high-frequency region, another unique spectral feature of ILs containing the  $[\text{NTf}_2]^-$  anion is the strong relative intensity band in the low-frequency region below 30  $\text{cm}^{-1}$ . This spectral feature has been confirmed not only in aromatic cation-based ILs, including imidazolium-based ILs,<sup>59,61,62,64,66,76</sup> but also in nonaromatic cation-based ILs, such as pyrrolidinium-based<sup>59</sup> and ammonium-based ILs.<sup>65</sup> Previously, Giraud et al.<sup>76</sup> and Rajian et al.<sup>68</sup> pointed out that the

Table 3. Fit Parameters and First Moments  $M_1$  for Low-Frequency Kerr Spectra in Dicationic and Monocationic ILs

(A) interionic vibrational band										
IL	$M_1$ (cm <sup>-1</sup> )	$a_0$	$\omega_0$ (cm <sup>-1</sup> )	$a_{G1}$	$\omega_{G1}$ (cm <sup>-1</sup> )	$\Delta\omega_{G1}$ (cm <sup>-1</sup> )	$a_{G2}$	$\omega_{G2}$ (cm <sup>-1</sup> )	$\Delta\omega_{G2}$ (cm <sup>-1</sup> )	$\Delta\omega_{G3}$ (cm <sup>-1</sup> )
[C <sub>6</sub> (MIm) <sub>2</sub> ][NTf <sub>2</sub> ] <sub>2</sub>	67.9	0.075 ± 0.001	3.5 ± 0.1	0.192 ± 0.062	10.7 ± 1.7	24.3 ± 2.4	0.117 ± 0.034	25.0 ± 6.2	37.8 ± 4.3	81.2 ± 0.3
[C <sub>10</sub> (MIm) <sub>2</sub> ][NTf <sub>2</sub> ] <sub>2</sub>	68.7	0.054 ± 0.001	3.7 ± 0.1	0.191 ± 0.068	9.9 ± 2.7	24.9 ± 2.6	0.124 ± 0.025	26.4 ± 4.9	41.9 ± 4.2	78.2 ± 0.5
[C <sub>12</sub> (MIm) <sub>2</sub> ][NTf <sub>2</sub> ] <sub>2</sub>	69.8	0.088 ± 0.001	2.7 ± 0.1	0.200 ± 0.083	8.9 ± 3.3	24.5 ± 2.7	0.119 ± 0.037	23.4 ± 7.5	43.8 ± 5.9	83.2 ± 0.6
[C <sub>3</sub> MIm][NTf <sub>2</sub> ]	69.5	0.139 ± 0.001	3.4 ± 0.1	0.297 ± 0.100	8.1 ± 3.1	24.5 ± 1.9	0.197 ± 0.036	24.7 ± 4.4	49.0 ± 4.2	88.3 ± 1.0
[C <sub>3</sub> MIm][NTf <sub>2</sub> ]	65.6	0.181 ± 0.001	2.3 ± 0.1	0.233 ± 0.093	6.6 ± 2.8	20.5 ± 1.6	0.229 ± 0.035	18.6 ± 3.3	42.6 ± 2.3	75.4 ± 0.2
[C <sub>6</sub> MIm][NTf <sub>2</sub> ]	68.0	0.115 ± 0.001	2.7 ± 0.1	0.175 ± 0.153	6.9 ± 5.5	20.5 ± 3.9	0.135 ± 0.028	19.7 ± 3.6	31.7 ± 2.2	92.5 ± 0.2
(B) intraionic vibrations										
IL	$a_{L1}$	$\omega_{L1}$ (cm <sup>-1</sup> )	$\Delta\omega_{L1}$ (cm <sup>-1</sup> )	$a_{L2}$	$\omega_{L2}$ (cm <sup>-1</sup> )	$\Delta\omega_{L2}$ (cm <sup>-1</sup> )	$a_{L3}$	$\omega_{L3}$ (cm <sup>-1</sup> )	$\Delta\omega_{L3}$ (cm <sup>-1</sup> )	
[C <sub>6</sub> (MIm) <sub>2</sub> ][NTf <sub>2</sub> ] <sub>2</sub>	4.44 ± 0.08	123.0 ± 0.2	7.0 ± 0.1	9.6 ± 0.4	172.9 ± 0.1	14.0 ± 0.2	54.5 ± 1.9	209.7 ± 0.2	32.3 ± 0.5	
[C <sub>10</sub> (MIm) <sub>2</sub> ][NTf <sub>2</sub> ] <sub>2</sub>	3.79 ± 0.08	122.7 ± 0.1	7.1 ± 0.1	13.6 ± 0.5	170.8 ± 0.1	16.8 ± 0.3	32.9 ± 1.1	211.2 ± 0.2	27.1 ± 0.4	
[C <sub>12</sub> (MIm) <sub>2</sub> ][NTf <sub>2</sub> ] <sub>2</sub>	1.90 ± 0.05	121.9 ± 0.1	5.4 ± 0.1	6.6 ± 0.4	171.6 ± 0.1	13.6 ± 0.3	80.4 ± 2.7	213.8 ± 0.3	40.5 ± 0.7	
[C <sub>3</sub> MIm][NTf <sub>2</sub> ]	4.61 ± 0.09	122.6 ± 0.1	6.8 ± 0.1	2.5 ± 0.1	171.1 ± 0.1	9.6 ± 0.2	43.7 ± 0.6	221.0 ± 0.1	29.5 ± 0.2	
[C <sub>3</sub> MIm][NTf <sub>2</sub> ]	2.06 ± 0.04	122.0 ± 0.1	5.5 ± 0.1	10.5 ± 0.3	169.9 ± 0.1	13.8 ± 0.2	61.2 ± 1.7	215.2 ± 0.3	39.5 ± 0.5	
[C <sub>6</sub> MIm][NTf <sub>2</sub> ]	1.82 ± 0.03	122.0 ± 0.1	5.5 ± 0.1	3.5 ± 0.2	171.5 ± 0.1	11.3 ± 0.2	34.6 ± 0.8	214.5 ± 0.2	32.6 ± 0.4	

Figure 7. Optimized structures of [C<sub>6</sub>(MIm)<sub>2</sub>]<sup>2+</sup> and [C<sub>3</sub>MIm]<sup>+</sup>. The calculation is based on the B3LYP/aug-cc-pVTZ level of theory.

interionic vibrational motion of the [NTf<sub>2</sub>]<sup>-</sup> anion contributes to the spectral intensity in this low-frequency region for imidazolium-based ILs containing the [NTf<sub>2</sub>]<sup>-</sup> anion. More recently, we have assigned this band primarily to the anion's libration or the coupling of translational and reorientational motions based on comparison with the spectra of 1-butyl-3-methylimidazolium-based ILs containing trifluoromethanesulfonate and tris(trifluoromethylsulfonyl)methide anions.<sup>66</sup> Also, it is worth notifying that the Kerr signal intensities of the imidazolium and the anion are stronger than those of the nonaromatic cations.

Because the [NTf<sub>2</sub>]<sup>-</sup> anion has two stable conformers, transoid and cisoid, it might be worth mentioning the anion structure in the dicationic ILs. It is reported that intraionic vibrational modes within the frequency range of 250–380 cm<sup>-1</sup> of the [NTf<sub>2</sub>]<sup>-</sup> anion, which are assigned to the intraionic modes containing rocking of CF<sub>3</sub> and twisting/wagging/rocking motions of SO<sub>2</sub> groups, are sensitive to the structure.<sup>64,109–112</sup> Also, it should be noted that the stable conformer structure of the [NTf<sub>2</sub>]<sup>-</sup> anion depends on the counteranion and the medium caused by the specific interionic interaction.<sup>64</sup> If the intraionic vibrational bands within the frequency range of 250–380 cm<sup>-1</sup> in Figures 4 and 5 are closed up, then it is obvious that there are few difference in the interionic vibrational bands between the dicationic and monocationic ILs. Accordingly, the spectral difference in both the intra- and interionic vibrations of the dicationic and monocationic ILs is negligibly influenced by the little geometric alteration of the [NTf<sub>2</sub>]<sup>-</sup> anion.

In brief summary, the present results show that the above-mentioned characteristic features of the low-frequency Kerr spectrum of imidazolium-based monocationic ILs containing the [NTf<sub>2</sub>]<sup>-</sup> anion also hold true for the present dicationic ILs; that is, the line-shape of the low-frequency Kerr spectrum of the dicationic imidazolium-based ILs containing the [NTf<sub>2</sub>]<sup>-</sup> anion is bimodal. Also, the stable anion structure in the dicationic ILs is not different from that in the corresponding monocationic ILs.

**4.2. Comparison of Low-Frequency Spectra between Dicationic and Monocationic ILs.** Comparison of the low-frequency Kerr spectra between the dicationic and monocationic ILs, based on the spectra presented in Figure 6, shows that overall the spectral profiles of the dicationic and monocationic ILs are modestly similar, except for the comparison between [C<sub>6</sub>(MIm)<sub>2</sub>][NTf<sub>2</sub>]<sub>2</sub> and [C<sub>3</sub>MIm][NTf<sub>2</sub>]. Accordingly, it can be expected that the microenvironments (or microstructures) of the ionic regions of the dicationic ILs of [C<sub>10</sub>(MIm)<sub>2</sub>][NTf<sub>2</sub>]<sub>2</sub> and [C<sub>12</sub>(MIm)<sub>2</sub>][NTf<sub>2</sub>]<sub>2</sub> are not very different from those of the



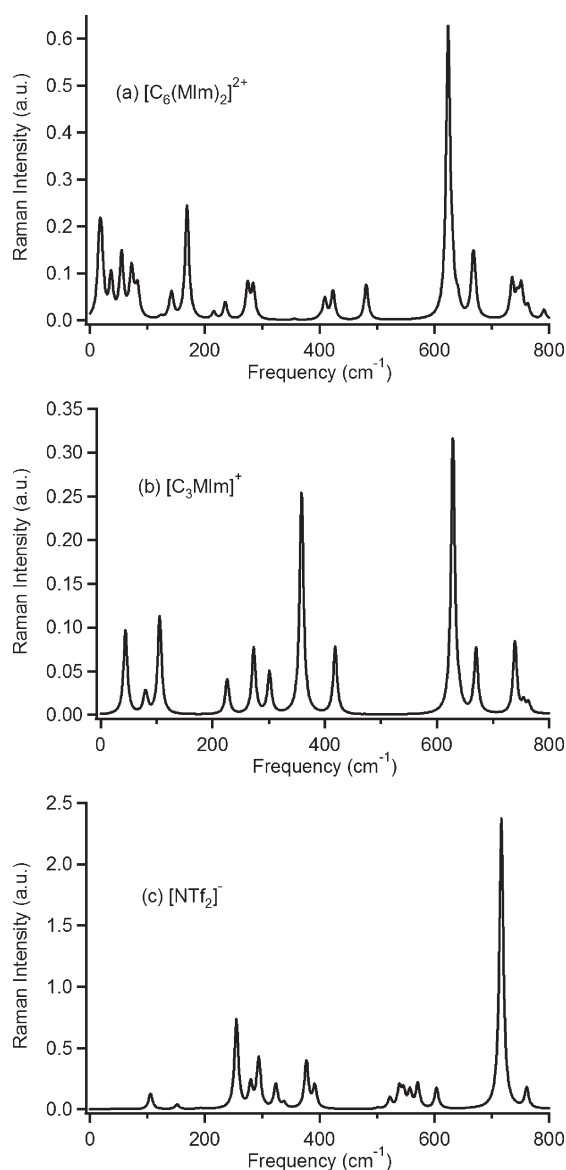


**Figure 8.** Raman spectra calculated for gas-phase (a)  $[\text{C}_6(\text{MIm})_2]^{2+}$ , (b)  $[\text{C}_3\text{MIm}]^+$ , and (c)  $[\text{NTf}_2]^-$  at the B3LYP/aug-cc-pVTZ level of theory.

monocationic ILs of  $[\text{C}_5\text{MIm}][\text{NTf}_2]$  and  $[\text{C}_6\text{MIm}][\text{NTf}_2]$ . Note that the low-frequency Kerr spectra of the imidazolium-based ILs with the  $[\text{NTf}_2]^-$  anion can be largely attributed to the interionic vibrations originating from the imidazolium ring and the anion but not arising from the alkyl group of the cation. In addition, the present results indicate that the alkylene linkers of the dications are unlikely rigid. Although the quantum chemical calculation results show that the polarizability anisotropy volume of the optimized  $[\text{C}_6(\text{MIm})_2]^{2+}$  dication is more than twice of that of the optimized  $[\text{C}_3\text{MIm}]^+$  cation, the quantum chemical calculation results do not correspond to the relative spectral intensity ratio of the dicationic and monocationic ILs. Furthermore, it is expected that the two imidazolium moieties in one dication could vibrate without interfering with each other because the interionic vibrational spectra of the dicationic and monocationic ILs are not very different.

However, upon close examination of the spectra, we observe a slight difference in the relative intensities of the dicationic ILs

( $[\text{C}_{10}(\text{MIm})_2][\text{NTf}_2]_2$  and  $[\text{C}_{12}(\text{MIm})_2][\text{NTf}_2]_2$ ) and the monocationic ILs ( $[\text{C}_5\text{MIm}][\text{NTf}_2]$  and  $[\text{C}_6\text{MIm}][\text{NTf}_2]$ ) in the low-frequency region (ca.  $17\text{ cm}^{-1}$ ) to the high-frequency region (ca.  $70\text{ cm}^{-1}$ ). The intensity ratio of the low-frequency region to the high-frequency region ( $I_l/I_h$ ) is 1.03 for  $[\text{C}_{10}(\text{MIm})_2][\text{NTf}_2]_2$ , 1.04 for  $[\text{C}_{12}(\text{MIm})_2][\text{NTf}_2]_2$ , 1.08 for  $[\text{C}_5\text{MIm}][\text{NTf}_2]$ , and 1.07 for  $[\text{C}_6\text{MIm}][\text{NTf}_2]$ , respectively. Previously, we have shown that the translational motions of the cation and the anion and the coupling motions of the translational and reorientational motions significantly influence the low-frequency region of the broad Kerr spectra of 1-butyl-3-methylimidazolium-based ILs with hexafluorophosphate anions using MD simulations.<sup>107</sup> Therefore, it is plausible that the translational motions of the dicationic ILs are suppressed by the alkylene linker in comparison with the monocationic ILs. A similar feature has also been reported in aqueous solutions of monomers and oligomers of amides and acids, where the relative intensity of the low-frequency region of the broad Kerr spectrum of the aqueous solutions decreases as the molecular weight of the amides and acids increases.<sup>113</sup> This is also true for the neat liquids and carbon tetrachloride solutions of 1,3-diphenylpropane and alkylbenzenes, which represent a more comparable system.<sup>86</sup> It should be recalled that the differences between the low-frequency Kerr spectra of the dicationic ILs  $[\text{C}_{10}(\text{MIm})_2][\text{NTf}_2]_2$  and  $[\text{C}_{12}(\text{MIm})_2][\text{NTf}_2]_2$  and those of the monocationic ILs  $[\text{C}_5\text{MIm}][\text{NTf}_2]$  and  $[\text{C}_6\text{MIm}][\text{NTf}_2]$  are not very large. This indicates that the translational motion activity, which affects the low-frequency Kerr spectrum, is not very different for the dicationic ILs and the corresponding monocationic ILs, and the motions of the two imidazolium rings of the single dication are largely independent of each other. It can also be expected that the microenvironments of the probed ions and ionic moieties (ionic region) in the dicationic ILs are similar to those in the monocationic ILs. Therefore, it is clear that the alkylene linker only weakly affects the interionic vibrations of the dicationic ILs. However, there is a marked difference in the low-frequency Kerr spectra of  $[\text{C}_6(\text{MIm})_2][\text{NTf}_2]_2$  and  $[\text{C}_3\text{MIm}][\text{NTf}_2]$ . This point is discussed in the next section.

**4.3. Dependences of Low-Frequency Spectrum on Alkylene Linker and Alkyl Group of Cations.** As shown in Figure 6, the line-shape of the low-frequency Kerr spectrum of  $[\text{C}_3\text{MIm}][\text{NTf}_2]$  is very different from those of  $[\text{C}_5\text{MIm}][\text{NTf}_2]$  and  $[\text{C}_6\text{MIm}][\text{NTf}_2]$ . Given that the interionic vibrational spectra probe the microscopic aspects of ILs, it is worth discussing the present results in combination with the information of the structure of neat ILs. There are several reports regarding the microstructure of ILs. MD simulation works by Lopes and Padua have shown the substantial nanostructural organizations in the ILs of  $[\text{C}_n\text{MIm}][\text{PF}_6]$ .<sup>78,79</sup> In their MD simulations, the degree of microphase separation was enhanced with increasing the alkyl chain length in the  $[\text{C}_n\text{MIm}]^+$  cation. Voth and coworkers have performed MD simulations demonstrating that both spatial aggregation and tail aggregation in  $[\text{C}_n\text{MIm}][\text{NO}_3]$  ILs<sup>80,81</sup> are in excellent qualitative agreement with the results of Lopes and Padua.<sup>78,79</sup> Recently, Balasubramanian and coworkers have carried out MD simulations for  $[\text{C}_n\text{MIm}][\text{PF}_6]$  ILs<sup>82</sup> and compared the scattering structure factors for solid  $[\text{C}_4\text{MIm}][\text{PF}_6]$  with the X-ray and neutron scattering data by Triolo and coworkers.<sup>114</sup> Experimentally, Shigeto and Hamaguchi have applied spatially resolved coherent anti-Stokes Raman spectroscopy to  $[\text{C}_n\text{MIm}][\text{PF}_6]$  ILs and have found a trace of the local structures on the order of tens of nanometers.<sup>83</sup> Using X-ray diffraction, Triolo et al. have clearly observed the evidence of the existence of nanoscale



heterogeneities in ILs of  $[C_n\text{MIm}]\text{Cl}$  and  $[C_n\text{MIm}][\text{BF}_4]$ .<sup>84</sup> They have also observed the similar evidence of  $[C_n\text{MIm}][\text{PF}_6]$  by X-ray diffraction.<sup>85</sup>

In 2009, Quitevis, Triolo, and coworkers compared the low-frequency Kerr spectra with the X-ray-scattering data for a series of 1-alkyl-3-methylimidazolium ILs containing the  $[\text{NTf}_2]^-$  anion.<sup>74</sup> The X-ray-scattering data in that study have shown that the scattering peak (in the  $Q$  range  $2\text{--}6\text{ nm}^{-1}$ ) arising from nanoscale segregation becomes more distinct as the length of the alkyl group of the  $[C_n\text{MIm}]^+$  cation increases, and the band becomes more ambiguous in the ILs of cations containing shorter alkyl groups. Close examination of their data (Figure 3 in ref 74) shows that the scattering intensity is almost negligible in the ILs of the cations of 1-ethyl-3-methylimidazolium and 1-methyl-3-propylimidazolium. Thus, it is likely that  $[C_3\text{MIm}][\text{NTf}_2]$  is relatively homogeneous but  $[C_5\text{MIm}][\text{NTf}_2]$  and  $[C_6\text{MIm}][\text{NTf}_2]$  exhibit nanoscale segregation structures. Accordingly, the unique spectral features of  $[C_3\text{MIm}][\text{NTf}_2]$  can be accounted for based on a difference in its microscopic structure relative to those of  $[C_5\text{MIm}][\text{NTf}_2]$  and  $[C_6\text{MIm}][\text{NTf}_2]$ . The observed larger relative intensity of the low-frequency region to the high-frequency region for  $[C_3\text{MIm}][\text{NTf}_2]$  compared with  $[C_5\text{MIm}][\text{NTf}_2]$  and  $[C_6\text{MIm}][\text{NTf}_2]$  seems to be reasonably explained by this consideration. The spectral difference between  $[C_3\text{MIm}][\text{NTf}_2]$  and the other two monocationic ILs possibly arises from the difference in the activities of the translational motions because translational motions contribute significantly to the low-frequency region of the broad interionic vibrational band in ILs. In the microsegregation structure, translational motions can be expected to be suppressed by the restricted structure. As a result, the relative intensities of the low-frequency region to the high-frequency region for  $[C_5\text{MIm}][\text{NTf}_2]$  and  $[C_6\text{MIm}][\text{NTf}_2]$  become lower than that for  $[C_3\text{MIm}][\text{NTf}_2]$ .

In contrast, the dependence of the spectral shapes on the alkylene linker for the dicationic ILs is not very large in comparison with the monocationic ILs. The spectral shapes for the dicationic ILs are more similar to those of  $[C_5\text{MIm}][\text{NTf}_2]$  and  $[C_6\text{MIm}][\text{NTf}_2]$  than that of  $[C_3\text{MIm}][\text{NTf}_2]$ . Although the liquid structures of the dicationic ILs have not yet been reported, it can be expected that the dicationic ILs studied here likely have nanoscale segregation structures similar to those of  $[C_5\text{MIm}][\text{NTf}_2]$  and  $[C_6\text{MIm}][\text{NTf}_2]$ . The lengths of the alkylene linkers in the dications are approximately twice as long as those of the alkyl groups in the corresponding monocations. The alkylene linkers of the dications (in particular,  $[C_6(\text{MIm})_2]^{2+}$ ) are likely to be long enough to facilitate the formation of nanoscale segregation structures. This is a similar concept of the hydrophobic interaction in aqueous systems. It is well known that the hydrophobic interaction becomes stronger with the longer alkyl chain. In ionic surfactants, the critical micelle concentration and the surfactant aggregation number increase with the alkyl group of the surfactants.<sup>115,116</sup> In the case of dicationic surfactants, Tamaki et al. studied the concentration dependence of the surface tension in aqueous solutions of several  $N,N'$ -polymethylenebis(trimethylammonium) dibromides and found that the surfactant having the alkylene linker of hexylene is a border salt and the surfactants having the longer alkylene linker are classified as hydrophobic structure makers.<sup>117</sup> They also reported the micelle formation of  $N,N'$ -dodecylenebis(trimethylammonium) dibromide in water at 298 K and estimated the critical micelle concentration of 0.07 M from the electrical conductivity measurements.<sup>117</sup> These facts remind us that the similar feature of the segregation

in ILs likely appears as well. The present study thus indicates that the hexylene linker is long enough to segregate in the dicationic IL. In contrast with the nonpolar region, the components of the ionic region involve the imidazolium rings and the anions for all present ILs. Because the low-frequency Kerr spectra of imidazolium-based ILs containing the  $[\text{NTf}_2]^-$  anion are dominated by the signals of the imidazolium ring and the anion, the low-frequency Kerr spectra primarily probe the ionic regions, and thus, the present results of the spectral profiles for the sample ILs imply that  $[C_3\text{MIm}][\text{NTf}_2]$ , whose propyl group is not long enough to segregate in the IL, is rather homogeneous, but the other ILs include the segregation structures. This feature comes from the fact that the dications include the imidazolium rings at both ends of the alkylene linker, whereas the monocations consist of the alkyl group and one imidazolium ring.

**4.4. Comparison of Low-Frequency Kerr Spectrum with Bulk Properties.** Before we conclude this study, brief remarks regarding the comparison of the low-frequency Kerr spectrum to the bulk properties in the dicationic ILs are given. Previously, the linear correlation between the first moment of the low-frequency Kerr spectrum and the value of the square root of the value of the surface tension divided by liquid density  $(\gamma/d)^{1/2}$  in 40 aprotic molecular liquids including 20 aromatic liquids and 20 nonaromatic liquids has been reported.<sup>52</sup> This fact indicates that the intermolecular force in molecular liquids is largely influenced by the intermolecular vibration that probes the microscopic intermolecular interaction. In the present ILs, the values of  $(\gamma/d)^{1/2}$  of the dicationic and monocationic ILs do not very depend on the lengths of alkylene linker and alkyl group and are approximately  $(5.2\text{ and }4.9) \times 10^{-3}\text{ m}^{3/2}\text{s}$ , respectively. On the basis of this correlation, it can be expected that the first moment of the low-frequency Kerr spectrum in the dicationic ILs is slightly higher frequency than that in the monocationic ILs. However, a clear difference in the first moment of the low-frequency Kerr spectrum between the dicationic and monocationic ILs was not confirmed, as shown in Table 3. As discussed in Sections 4.1 and 4.3, the low-frequency Kerr spectrum originates mainly from the interionic vibrational motions of the imidazolium moieties and the anions, and the ILs, except for  $[C_3\text{MIm}][\text{NTf}_2]$ , include the microsegregation structures. As a result, the microscopic interionic interaction in the ILs probed by the interionic vibrational spectrum does not linearly correlate to the bulk intermolecular force. In other words, the information on the ionic region in heterogeneous structure ILs observed by the low-frequency Kerr spectrum is emphasized in contrast with the nonpolar region.

## 5. CONCLUSIONS

In this study, the interionic vibrations of imidazolium-based dicationic ILs and the reference monocationic ILs were closely compared using the femtosecond OHD-RIKES technique. In general, the low-frequency Kerr spectra of the dicationic ILs are not very different from those of the corresponding monocationic ILs, except for the case of the comparison between the ILs whose cations have a shorter alkylene linker or alkyl group:  $[C_6(\text{MIm})_2][\text{NTf}_2]_2$  and  $[C_3\text{MIm}][\text{NTf}_2]$ . Detailed inspection of the Kerr spectra, however, reveals small differences in the relative intensities of the low-frequency component to the higher-frequency component for the broad Kerr spectra: the relative intensities of the low-frequency components are slightly smaller for the dicationic ILs than for the monocationic ILs. It was also found that the spectral profiles (line-shapes) of the dicationic ILs do not

vary significantly, but the spectrum of  $[\text{C}_3\text{MIm}][\text{NTf}_2]$  is very different from those of the other monocationic ILs. With reference to the X-ray scattering data,<sup>74</sup> these features are attributed to the difference in the microstructures of the ILs:  $[\text{C}_3\text{MIm}][\text{NTf}_2]$  is rather homogeneous, but the dicationic ILs and the other monocationic ILs contain the segregation structures. Unlike simple molecular liquids, the parameter of the bulk properties, the square root of the value of the surface tension divided by liquid density  $(\gamma/d)^{1/2}$ , in the ILs is insensitive to the first moment of the low-frequency Kerr spectrum. This could arise from the microsegregation structures of the ILs. In the near future, we hope to provide a more in-depth analysis of the molecular aspects of the interionic vibrations and the microstructures in dicationic ILs using MD simulations.

## ■ ASSOCIATED CONTENT

**S Supporting Information.** Ab initio quantum chemical calculation results (atom coordinates, polarizability tensor elements, mean polarizabilities, and polarizability anisotropy volumes). This material is available free of charge via the Internet at <http://pubs.acs.org>.

## ■ AUTHOR INFORMATION

### Corresponding Author

\*E-mail: [shiota@faculty.chiba-u.jp](mailto:shiota@faculty.chiba-u.jp), [ishida@ims.ac.jp](mailto:ishida@ims.ac.jp).

## ■ ACKNOWLEDGMENT

This work was partially supported by the Ministry of Education, Culture, Sports, Science and Technology (MEXT) of Japan (Grant-in-Aid for Young Scientists (A): 21685001 to H.S. and Grant-in-Aid for Scientific Research (C): 23550029 to T.I.), the Futaba Electronics Memorial Foundation, and the Iwatani Naoji Foundation.

## ■ REFERENCES

- (1) *Ionic Liquids in Synthesis*, 2nd ed.; Wasserscheid, P., Welton, T., Eds.; Wiley-VCH: Weinheim, Germany, 2008.
- (2) *Electrochemical Aspects of Ionic Liquids*; Ohno, H., Ed.; Wiley-Interscience: Hoboken, NJ, 2005.
- (3) *Ionic Liquids: Theory, Properties, New Approaches*; Kokorin, A., Ed.; InTech: Rijeka, Croatia, 2011.
- (4) *Ionic Liquids: Applications and Perspectives*; Kokorin, A., Ed.; InTech: Rijeka, Croatia, 2011.
- (5) Welton, T. *Chem. Rev.* **1999**, 99, 2071.
- (6) Weingaertner, H. *Angew. Chem., Int. Ed.* **2008**, 47, 654.
- (7) Plechkova, N. V.; Seddon, K. R. *Chem. Soc. Rev.* **2008**, 37, 123.
- (8) Ohno, H.; Fukumoto, K. *Electrochemistry* **2008**, 76, 16.
- (9) Wishart, J. F. *Energy Environ. Sci.* **2009**, 2, 967.
- (10) Wilkes, J. S.; Zaworotko, M. J. *J. Chem. Soc., Chem. Commun.* **1992**, 965.
- (11) Wilkes, J. S. *Green Chem.* **2002**, 4, 73.
- (12) Deetlefs, M.; Seddon, K. R. *Chem. Today* **2006**, 24, 16.
- (13) Rogers, R. D.; Voth, G. A. *Acc. Chem. Res.* **2007**, 40, 1077.
- (14) Hough, W. L.; Rogers, R. D. *Bull. Chem. Soc. Jpn.* **2007**, 80, 2262.
- (15) Kobrak, M. N. *Adv. Chem. Phys.* **2008**, 139, 85.
- (16) Armand, M.; Endres, F.; MacFarlane, D. R.; Ohno, H.; Scrosati, B. *Nat. Mater.* **2009**, 8, 621.
- (17) Samanta, A. *J. Phys. Chem. Lett.* **2010**, 1, 1557.
- (18) Castner, E. W., Jr.; Wishart, J. F. *J. Chem. Phys.* **2010**, 132, 120901.
- (19) Engel, R.; Cohen, J. I. *Curr. Org. Chem.* **2002**, 6, 1453.
- (20) Lall, S. I.; Mancheno, D.; Castro, S. B.; V.; Cohen, J. I.; Engel, R. *Chem. Commun.* **2000**, 2413.
- (21) Engel, R.; Cohen, J. I.; Lall, S. I. *Phosphorus, Sulfur Silicon Relat. Elem.* **2000**, 177, 1441.
- (22) Lall, S.; Behaj, V.; Mancheno, D.; Casiano, R.; Thomas, M.; Rikin, A.; Gaillard, J.; Raju, R.; Scumpia, A.; Castro, S.; Engel, R.; Cohen, J. I. *Synthesis* **2002**, 1530.
- (23) Wishart, J. F.; Lall-Ramnarine, S. I.; Raju, R.; Scumpia, A.; Bellevue, S.; Ragbir, R.; Engel, R. *Radiat. Phys. Chem.* **2005**, 72, 99.
- (24) Ito, K.; Nishina, N.; Ohno, H. *Electrochim. Acta* **2000**, 45, 1295.
- (25) Yoshizawa, M.; Ito-Akita, K.; Ohno, H. *Electrochim. Acta* **2000**, 45, 1617.
- (26) Anderson, J. L.; Ding, R.; Ellern, A.; Armstrong, D. W. *J. Am. Chem. Soc.* **2005**, 127, 593.
- (27) Ding, Y.-S.; Zhaa, M.; Zhang, J.; Wang, S.-S. *Colloids Surf., A* **2007**, 298, 201.
- (28) Pitawala, J.; Matic, A.; Martinelli, A.; Jacobsson, P.; Koch, V.; Croce, F. *J. Phys. Chem. B* **2009**, 113, 10607.
- (29) Lee, M.; Niu, Z.; Slebodnick, C.; Gibson, H. W. *J. Phys. Chem. B* **2010**, 114, 7312.
- (30) Wang, R.; Jin, C.-M.; Twamley, B.; Shreeve, J. M. *Inorg. Chem.* **2006**, 45, 6396.
- (31) Wang, R.; Gao, H.; Ye, C.; Shreeve, J. M. *Chem. Mater.* **2007**, 19, 144.
- (32) Payagala, T.; Huang, J.; Breitbach, Z. S.; Sharma, P. S.; Armstrong, D. W. *Chem. Mater.* **2007**, 19, 5848.
- (33) Shiota, H.; Mandai, T.; Fukazawa, H.; Kato, T. *J. Chem. Eng. Data* **2011**, 56, 2453.
- (34) Jin, C.-M.; Ye, C.; Phillips, B. S.; Zabinski, J. S.; Liu, X.; Liu, W.; Shreeve, J. M. *J. Mater. Chem.* **2006**, 16, 1529.
- (35) Zeng, Z.; Phillips, B. S.; Xiao, J.-C.; Shreeve, J. M. *Chem. Mater.* **2008**, 20, 2719.
- (36) Yu, G.; Yan, S.; Zhou, F.; Liu, X.; Liu, W.; Liang, Y. *Tribol. Lett.* **2007**, 25, 197.
- (37) Palacio, M.; Bhushan, B. *J. Vac. Sci. Technol., A* **2009**, 27, 986.
- (38) Anderson, J. L.; Armstrong, D. W. *Anal. Chem.* **2005**, 77, 6453.
- (39) Qi, M.; Armstrong, D. W. *Anal. Bioanal. Chem.* **2007**, 388, 889.
- (40) Huang, K.; Han, X.; Zhang, X.; Armstrong, D. W. *Anal. Bioanal. Chem.* **2007**, 389, 2265.
- (41) Han, X.; Armstrong, D. W. *Org. Lett.* **2005**, 7, 4205.
- (42) Zhang, Z.; Zhou, H.; Yang, L.; Tachibana, K.; Kamijima, K.; Xu, J. *Electrochim. Acta* **2008**, 53, 4833.
- (43) Kim, J. Y.; Kim, T. H.; Kim, D. Y.; Park, N.-G.; Ahn, K.-D. *J. Power Sources* **2008**, 175, 692.
- (44) Zafera, C.; Ocakoglu, K.; Ozsoy, C.; Icli, S. *Electrochim. Acta* **2009**, 54, 5709.
- (45) McMorrow, D.; Lotshaw, W. T.; Kenney-Wallace, G. A. *IEEE J. Quantum Electron.* **1988**, 24, 443.
- (46) Lotshaw, W. T.; McMorrow, D.; Thant, N.; Melinger, J. S.; Kitchenham, R. *J. Raman Spectrosc.* **1995**, 26, 571.
- (47) Righini, R. *Science* **1993**, 262, 1386.
- (48) Kinoshita, S.; Kai, Y.; Ariyoshi, T.; Shimada, Y. *Int. J. Mod. Phys. B* **1996**, 10, 1229.
- (49) Castner, E. W., Jr.; Maroncelli, M. *J. Mol. Liq.* **1998**, 77, 1.
- (50) Smith, N. A.; Meech, S. R. *Int. Rev. Phys. Chem.* **2002**, 21, 75.
- (51) Zhong, Q.; Fourkas, J. T. *J. Phys. Chem. B* **2008**, 112, 15529.
- (52) Shiota, H.; Fujisawa, T.; Fukazawa, H.; Nishikawa, K. *Bull. Chem. Soc. Jpn.* **2009**, 82, 1347.
- (53) Heisler, I. A.; Meech, S. R. *Science* **2010**, 327, 857.
- (54) Loughnane, B. J.; Farrer, R. A.; Scodinu, A.; Reilly, T.; Fourkas, J. T. *J. Phys. Chem. B* **2000**, 104, 5421.
- (55) Farrer, R. A.; Fourkas, J. T. *Acc. Chem. Res.* **2003**, 36, 605.
- (56) Hunt, N. T.; Jaye, A. A.; Meech, S. R. *Phys. Chem. Chem. Phys.* **2007**, 9, 2167.
- (57) Shiota, H.; Fukazawa, H. Atom Substitution Effects in Ionic Liquids: A Microscopic View by Femtosecond Raman-Induced Kerr Effect Spectroscopy. In *Ionic Liquids: Theory, Properties, New Approaches*; Kokorin, A., Ed.; InTech: Rijeka, Croatia, 2011; p 201.

- (58) Castner, E. W., Jr.; Wishart, J. F.; Shirota, H. *Acc. Chem. Res.* **2007**, *40*, 1217.
- (59) Shirota, H.; Funston, A. M.; Wishart, J. F.; Castner, E. W., Jr. *J. Chem. Phys.* **2005**, *122*, 184512.
- (60) Shirota, H.; Castner, E. W., Jr. *J. Phys. Chem. A* **2005**, *109*, 9388.
- (61) Shirota, H.; Castner, E. W., Jr. *J. Phys. Chem. B* **2005**, *109*, 21576.
- (62) Shirota, H.; Wishart, J. F.; Castner, E. W., Jr. *J. Phys. Chem. B* **2007**, *111*, 4819.
- (63) Shirota, H.; Nishikawa, K.; Ishida, T. *J. Phys. Chem. B* **2009**, *113*, 9831.
- (64) Fujisawa, T.; Nishikawa, K.; Shirota, H. *J. Chem. Phys.* **2009**, *131*, 244519.
- (65) Shirota, H.; Fukazawa, H.; Fujisawa, T.; Wishart, J. F. *J. Phys. Chem. B* **2010**, *114*, 9400.
- (66) Fukazawa, H.; Ishida, T.; Shirota, H. *J. Phys. Chem. B* **2011**, *115*, 4621.
- (67) Hyun, B. R.; Dzyuba, S. V.; Bartsch, R. A.; Quitevis, E. L. *J. Phys. Chem. A* **2002**, *106*, 7579.
- (68) Rajian, J. R.; Li, S. F.; Bartsch, R. A.; Quitevis, E. L. *Chem. Phys. Lett.* **2004**, *393*, 372.
- (69) Xiao, D.; Rajian, J. R.; Li, S. F.; Bartsch, R. A.; Quitevis, E. L. *J. Phys. Chem. B* **2006**, *110*, 16174.
- (70) Xiao, D.; Rajian, J. R.; Cady, A.; Li, S.; Bartsch, R. A.; Quitevis, E. L. *J. Phys. Chem. B* **2007**, *111*, 4669.
- (71) Xiao, D.; Rajian, J. R.; Hines, L. G., Jr.; Li, S.; Bartsch, R. A.; Quitevis, E. L. *J. Phys. Chem. B* **2008**, *112*, 13316.
- (72) Xiao, D.; Hines, L. G., Jr.; Bartsch, R. A.; Quitevis, E. L. *J. Phys. Chem. B* **2009**, *113*, 4544.
- (73) Xiao, D.; Hines, L. G., Jr.; Li, S.; Bartsch, R. A.; Quitevis, E. L.; Russina, O.; Triolo, A. *J. Phys. Chem. B* **2009**, *113*, 6426.
- (74) Russina, O.; Triolo, A.; Gontrani, L.; Caminiti, R.; Xiao, D.; Hines, L. G., Jr.; Bartsch, R. A.; Quitevis, E. L.; Plechkova, N.; Seddon, K. R. *J. Phys.: Condens. Matter* **2009**, *21*, 424121.
- (75) Xiao, D.; Hines, L. G., Jr.; Holtz, M. W.; Song, K.; Bartsch, R. A.; Quitevis, E. L. *Chem. Phys. Lett.* **2010**, *497*, 37.
- (76) Giraud, G.; Gordon, C. M.; Dunkin, I. R.; Wynne, K. *J. Chem. Phys.* **2003**, *119*, 464.
- (77) Turton, D. A.; Hunger, J.; Stoppa, A.; Hefter, G.; Thoman, A.; Walther, M.; Buchner, R.; Wynne, K. *J. Am. Chem. Soc.* **2009**, *131*, 11140.
- (78) Lopes, J. N. A. C.; Padua, A. A. H. *J. Phys. Chem. B* **2006**, *110*, 3330.
- (79) Lopes, J. N. C.; Gomes, M. F. C.; Padua, A. A. H. *J. Phys. Chem. B* **2006**, *110*, 16816.
- (80) Wang, Y.; Voth, G. A. *J. Am. Chem. Soc.* **2005**, *127*, 12192.
- (81) Wang, Y.; Voth, G. A. *J. Phys. Chem. B* **2006**, *110*, 18601.
- (82) Bhargava, B. L.; Devane, R.; Klein, M. L.; Balasubramanian, S. *Soft Matter* **2007**, *3*, 1395.
- (83) Shiget, S.; Hamaguchi, H.-o. *Chem. Phys. Lett.* **2006**, *427*, 329.
- (84) Triolo, A.; Russina, O.; Bleif, H.-J.; Di Cola, E. *J. Phys. Chem. B* **2007**, *111*, 4641.
- (85) Triolo, A.; Russina, O.; Fazio, B.; Triolo, R.; Cola, E. D. *Chem. Phys. Lett.* **2008**, *457*, 362.
- (86) Shirota, H. *J. Chem. Phys.* **2005**, *122*, 044514.
- (87) Becke, A. D. *J. Chem. Phys.* **1993**, *98*, 5648.
- (88) Lee, C.; Yang, W.; Parr, R. G. *Phys. Rev. B* **1988**, *37*, 785.
- (89) Dunning, T. H., Jr. *J. Chem. Phys.* **1989**, *90*, 1007.
- (90) Kendall, R. A.; Dunning, T. H., Jr.; Harrison, R. J. *J. Chem. Phys.* **1992**, *96*, 6796.
- (91) Woon, D. E.; Dunning, T. H., Jr. *J. Chem. Phys.* **1993**, *98*, 1358.
- (92) Frisch, M. J.; Trucks, G. W.; Schlegel, H. B.; Scuseria, G. E.; Robb, M. A.; Cheeseman, J. R.; Montgomery, J. A., Jr.; Vreven, T.; Kudin, K. N.; Barone, V.; Mennucci, B.; Cossi, M.; Scalmani, G.; Rega, N.; Petersson, G. A.; Nakatsuji, H.; Hada, M.; Ehara, M.; Toyota, K.; Fukuda, R.; Hasegawa, J.; Ishida, M.; Nakajima, T.; Honda, Y.; Kitao, O.; Nakai, H.; Klene, M.; Li, X.; Knox, J. E.; Hratchian, H. P.; Cross, J. B.; Adamo, C.; Jaramillo, J.; Gomperts, R.; Stratmann, R. E.; Yazyev, O.; Austin, A. J.; Cammi, R.; Pomelli, C.; Ochterski, J. W.; Ayala, P. Y.; Morokuma, K.; Voth, G. A.; Salvador, P.; Dannenberg, J. J.; Zakrzewski, V. G.; Dapprich, S.; Daniels, A. D.; Strain, M. C.; Farkas, O.; Malick, D. K.; Rabuck, A. D.; Raghavachari, K.; Foresman, J. B.; Ortiz, J. V.; Cui, Q.; Baboul, A. G.; Clifford, S.; Cioslowski, J.; Stefanov, B. B.; Liu, G.; Liashenko, A.; Piskorz, P.; Komaromi, I.; Martin, R. L.; Fox, D. J.; Keith, T.; Al-Laham, M. A.; Peng, C. Y.; Nanayakkara, A.; Challacombe, M.; Gill, P. M. W.; Johnson, B.; Chen, W.; Wong, M. W.; Gonzalez, C.; Pople, J. A. *Gaussian 03*; Gaussian, Inc.: Pittsburgh, PA, 2003.
- (93) Cang, H.; Li, J.; Fayer, M. D. *J. Chem. Phys.* **2003**, *119*, 13017.
- (94) Li, J.; Wang, L.; Fruchey, K.; Fayer, M. D. *J. Phys. Chem. A* **2006**, *110*, 10384.
- (95) McMorro, D.; Lotshaw, W. T. *Chem. Phys. Lett.* **1990**, *174*, 85.
- (96) McMorro, D.; Lotshaw, W. T. *J. Phys. Chem.* **1991**, *95*, 10395.
- (97) Chang, Y. J.; Castner, E. W., Jr. *J. Chem. Phys.* **1993**, *99*, 7289.
- (98) Bodo, E.; Caminiti, R. *J. Phys. Chem. A* **2010**, *114*, 12506.
- (99) McMorro, D.; Lotshaw, W. T. *Chem. Phys. Lett.* **1993**, *201*, 369.
- (100) Cong, P.; Simon, J. D.; She, C. Y. *J. Chem. Phys.* **1996**, *104*, 962.
- (101) Smith, N. A.; Lin, S. J.; Meech, S. R.; Shirota, H.; Yoshihara, K. *J. Phys. Chem. A* **1997**, *101*, 9578.
- (102) Smith, N. A.; Meech, S. R. *J. Phys. Chem. A* **2000**, *104*, 4223.
- (103) Ronne, C.; Jensby, K.; Loughnane, B. J.; Fourkas, J.; Fauskov Nielsen, O.; Keiding, S. R. *J. Chem. Phys.* **2000**, *113*, 3749.
- (104) Manfred, K.; He, X.; Fourkas, J. T. *J. Phys. Chem. B* **2010**, *114*, 12096.
- (105) Urahata, S. M.; Ribeiro, M. C. C. *J. Chem. Phys.* **2005**, *122*, 024511.
- (106) Hu, Z.; Huang, X.; Annapureddy, H. V. R.; Margulis, C. J. *J. Phys. Chem. B* **2008**, *112*, 7837.
- (107) Ishida, T.; Nishikawa, K.; Shirota, H. *J. Phys. Chem. B* **2009**, *113*, 9840.
- (108) Sarangi, S. S.; Reddy, S. K.; Balasubramanian, S. *J. Phys. Chem. B* **2011**, *115*, 1874.
- (109) Rey, I.; Johansson, P.; Lindgren, J.; Lassegues, J. C.; Grondin, J.; Servant, L. *J. Phys. Chem. A* **1998**, *102*, 3249.
- (110) Herstedt, M.; Smirnov, M.; Johansson, P.; Chami, M.; Grondin, J.; Servant, L.; Lassegues, J. C. *J. Raman Spectrosc.* **2005**, *36*, 762.
- (111) Lassegues, J. C.; Grondin, J.; Holomb, R.; Johansson, P. *J. Raman Spectrosc.* **2007**, *38*, 551.
- (112) Fujii, K.; Fujimori, T.; Takamuku, T.; Kanzaki, R.; Umebayashi, Y.; Ishiguro, S.-I. *J. Phys. Chem. B* **2006**, *110*, 8179.
- (113) Shirota, H.; Ushiyama, H. *J. Phys. Chem. B* **2008**, *112*, 13542.
- (114) Triolo, A.; Mandanici, A.; Russina, O.; Rodriguez-Mora, V.; Cutroni, M.; Hardacre, C.; Nieuwenhuyzen, M.; Bleif, H.-J.; Keller, L.; Ramos, M. A. *J. Phys. Chem. B* **2006**, *110*, 21357.
- (115) Israelachvili, J. N. *Intermolecular and Surface Forces*, 2nd ed.; Academic Press: London, 1992.
- (116) Tamoto, Y.; Segawa, H.; Shirota, H. *Langmuir* **2005**, *21*, 3757.
- (117) Tamaki, K.; Ohhara, Y.; Ogawa, N.; Domae, Y.; Kurokawa, T. *Bull. Chem. Soc. Jpn.* **1994**, *67*, 2867.